Original Articles

Overexpression of 1-Acyl-Glycerol-3-Phosphate Acyltransferase-α Enhances Lipid Storage in Cellular Models of Adipose Tissue and Skeletal Muscle

Hong Ruan and Henry J. Pownall

Plasma nonesterified fatty acids (NEFA) at elevated concentrations antagonize insulin action and thus may play a critical role in the development of insulin resistance in type 2 diabetes. Plasma NEFA and glucose concentrations are regulated, in part, by their uptake into peripheral tissues. Cellular energy uptake can be increased by enhancing either energy transport or metabolism. The effects of overexpression of 1-acylglycerol-3-phosphate acyltransferase (AGAT)-α, which catalyzes the second step in triglyceride formation from glycerol-3-phosphate, was studied in 3T3-L1 adipocytes and C2C12 myotubes. In myotubes, overexpression of AGAT-α did not affect total [^{14}C]glucose uptake in the presence or absence of insulin, whereas insulin-stimulated [^{14}C]glucose conversion to cellular lipids increased significantly (33%, $P = 0.004$) with a concomitant decrease (–30%, $P = 0.005$) in glycogen formation. [^{3}H]oleic acid (OA) uptake in AGAT-overexpressing myotubes increased 34% ($P = 0.027$) upon insulin stimulation. AGAT-α overexpression in adipocytes increased basal (130%, $P = 0.04$) and insulin-stimulated (27%, $P = 0.01$) [^{3}H]OA uptake, increased insulin-stimulated glucose uptake (56%, $P = 0.04$) and conversion to cellular lipids (85%, $P = 0.007$), and suppressed basal (–44%, $P = 0.01$) and isoproterenol-stimulated OA release (–45%, $P = 0.03$) but not glycerol release. Our data indicate that an increase in metabolic flow to triglyceride synthesis can inhibit NEFA release, increase NEFA uptake, and promote insulin-mediated glucose utilization in 3T3-L1 adipocytes. In myotubes, however, AGAT-α overexpression does not increase basal cellular energy uptake, but can enhance NEFA uptake and divert glucose from glycogen synthesis to lipogenesis upon insulin stimulation. *Diabetes* 50:233–240, 2001

From the Section of Atherosclerosis and Lipoprotein Research (H.J.P., H.R.), Department of Medicine, Baylor College of Medicine; and The Methodist Hospital (H.J.P.), Houston, Texas.

Address correspondence and reprint requests to Henry J. Pownall, PhD, Department of Medicine, MS A-601, Baylor College of Medicine, 6565 Fannin St., Houston, TX 77030. E-mail: hpownall@bcm.tmc.edu.

Received for publication 28 October 1999 and accepted in revised form 23 October 2000.

AGAT, 1-acylglycerol-3-phosphate acyltransferase; BSA, bovine serum albumin; DG, diglyceride; DMEM, Dulbecco's minimum essential medium; FACS, fatty acyl-CoA synthase; FATP, fatty acid transport protein; FITC, fluorescein isothiocyanate; GPAT, glycerol-3-phosphate acyltransferase; HSL, hormone-sensitive lipase; KRBH, Krebs-Ringer bicarbonate HEPES buffer; LPA, lysophosphatidic acid; NEFA, nonesterified fatty acids; OA, oleic acid; PA, phosphatidic acid; PBS, phosphate-buffered saline; PCR, polymerase chain reaction; TG, triglyceride; TLC, thin-layer chromatography.

Type 2 diabetes is characterized, in part, by excess energy as glucose and nonesterified fatty acids (NEFA) within the plasma compartment. Moreover, an elevated plasma NEFA concentration has been increasingly recognized as a systemic mediator of insulin resistance in type 2 diabetes (1–5). Excess plasma NEFA can inhibit insulin-stimulated glucose utilization in muscle (1–4) and promote hepatic production of glucose (4–6) and VLDL triglyceride (TG) (7,8). Acute systemic administration of NEFA inhibits glucose disposal in muscle in a dose-dependent fashion (4) and increases hepatic glucose output (5,6). Reduction of plasma NEFA concentration improves glucose utilization (9–11), enhances the suppression of hepatic glucose production by insulin (12), and reduces hyperinsulinemia in patients with type 2 diabetes (13). Thus, plasma NEFA elevation may be mechanistically linked to the cluster of metabolic abnormalities seen in type 2 diabetes, including hyperglycemia, hyperinsulinemia, and dyslipidemia.

Skeletal muscle and adipose tissue are major sites of energy utilization. Most of the glucose and NEFA taken up by resting muscle is converted to glycogen (14) and TG (15). Because of its mass, skeletal muscle is a significant storage site for excess plasma NEFA in patients with type 2 diabetes (16) and in animal models of the disease (17,18). However, the accumulation of intramuscular TG may increase lipid oxidation and decrease glucose uptake and insulin sensitivity (18,19). In contrast, increasing NEFA and glucose uptake in adipose tissue could reduce systemic NEFA availability and would eventually improve insulin sensitivity in liver and muscle.

Energy uptake can be increased by enhancing either of the proposed rate-limiting steps of energy utilization, i.e., energy transport across the plasma membrane or energy metabolism within the cell. Indeed, an increase in glucose transport (20–22) or metabolism (23,24) promotes glucose utilization in cultured cells and transgenic animals. Moreover, glucose metabolism appears to be rate limiting under conditions of enhanced glucose transport (22,25–29). Less is known about the regulation of NEFA uptake. Overexpression of long-chain fatty acid transport protein (FATP) increases NEFA uptake in 3T3-L1 fibroblasts (30). On the other hand, an increase in cytoplasmic fatty acyl-CoA synthase (FACS) activity without a change in FATP is sufficient to increase NEFA uptake (30), indicating that NEFA transport is not rate limiting and that intracellular NEFA metabolism can drive NEFA uptake.

Because insulin promotes energy uptake in adipose tissue and muscle, and because the ultimate effect of insulin is to enhance energy storage, we hypothesized that an increase in energy flow to TG synthesis would enhance cellular uptake of NEFA and, under certain conditions, glucose as well.

Four enzymes are involved in TG synthesis from glycerol-3-phosphate and fatty acyl-CoA (31). The second step in TG formation is catalyzed by 1-acylglycerol-3-phosphate acyltransferase (AGAT), which converts 1-acylglycerol-3-phosphate (lysophosphatidic acid) (LPA) to 1,2-diacylglycerol-3-phosphate (phosphatidic acid) (PA). AGAT occurs as α and β isoforms (32), which are expressed at high levels in adipose tissue and skeletal muscle (H.R. and H.J.P., unpublished data). To study the effects of AGAT-α on cellular TG synthesis and uptake of NEFA and glucose, we established stable 3T3-L1 and C2C12 cell lines representing adipose tissue and skeletal muscle, respectively, which overexpress AGAT-α. Herein, we report those effects.

RESEARCH DESIGN AND METHODS

Cell culture. 3T3-L1 cells were purchased from the American Type Culture Collection (Rockville, MD), maintained as fibroblasts, and differentiated into adipocytes as previously described (33). C2C12 myoblasts, obtained from Robert J. Schwartz, PhD, were maintained in Dulbecco's minimum essential medium (DMEM) supplemented with 10% fetal calf serum. After confluence, the culture medium was changed to DMEM with 2% horse serum to initiate myogenic differentiation. Before each assay, both 3T3-L1 adipocytes and C2C12 myotubes were serum starved for 3 h in Krebs-Ringer bicarbonate buffer solution with 25 mmol/l Krebs-Ringer bicarbonate HEPES buffer (KRBH) (pH 7.4) containing 100 µmol/l bovine serum albumin (BSA) (Sigma, St. Louis, MO) essentially fatty acid free, and 5 mmol/l glucose.

Stable cell lines. A 2,083-bp cDNA clone encoding human AGAT was isolated from a human adipocyte cDNA library (Clontech, Palo Alto, CA) using a human infant brain expressed sequence tag similar to yeast AGAT (GenBank no. T77083; Genome Systems, St. Louis, MO) as a hybridization probe. The cDNA clone contains an 852-bp open reading frame encoding a protein of 283 amino acids with a calculated molecular mass of 31.7 kDa. Membrane preparations from AGAT-deficient *Escherichia coli* strain JC-201 (34) transformed with full-length AGAT cDNA exhibited AGAT activity (H.R. and H.J.P., unpublished data). This AGAT was identical to the α isoform described by West et al. (32).

The polymerase chain reaction (PCR) method was used to delete the predicted NH_2-terminal 30–amino acid leader sequence of AGAT-α protein and to introduce an *Eco*RI site into the upstream sequence and a *Not*I site into the downstream sequence of AGAT-α. The resulting PCR fragment was subcloned into the pcDNA3.1/HisC vector (Invitrogen, Carlsbad, CA); its sequence was verified by DNA sequencing. The recombinant plasmid, pHis-AGAT, encodes 293 amino acids containing a 40–amino acid NH_2-terminal epitope tag (including six histidines) and has a calculated mass of 32.3 kDa. This expression construct was transfected into 3T3-L1 fibroblasts and C2C12 myoblasts using SuperFect reagent (Qiagen, Valencia, CA). After selection in G-418, pools of 40–60 surviving colonies were expanded for study. Control cell lines were transfected with pcDNA/HisC vector without the insert, followed by G-418 selection. Cell line expression of AGAT-α was confirmed by Western blot analysis and immunofluorescence microscopy using a monoclonal anti-His_6 antibody (Clontech). The transfection and selection were repeated, and the independent G-418–resistant clones were amplified and verified for AGAT expression by reverse-transcriptase–PCR and/or Western blot analysis. Phenotypes from the two selections were not distinguishable, and data are representative of the two selections.

Western blotting. Either 30 or 60 µg of total cellular protein was separated by 12% SDS-PAGE and electroblotted onto a nitrocellulose membrane (Amersham, Arlington Heights, IL). The filter was incubated for 1 h at room temperature with monoclonal anti-His_6 antibody (1:5,000; Clontech), washed, and incubated with horseradish peroxidase–conjugated secondary antibody. Bound antibodies were detected by using the enhanced chemiluminescence Western blotting analysis system (Amersham).

Immunofluorescence microscopy. Cells were grown on cover slips, fixed with 4% paraformaldehyde, permeabilized with 0.1% Triton X-100, washed with phosphate-buffered saline (PBS), blocked with 1% normal goat serum in PBS, and incubated for 1 h at room temperature with monoclonal anti-His_6 antibodies (1:500; Clontech). Cells were washed with PBS and incubated with fluorescein isothiocyanate (FITC) or rhodamine-conjugated goat anti–mouse IgG (Pierce, Rockford, IL). Cells were treated with 4,6-diamidino-2-phenylindole as a counterstain, washed extensively with PBS, and examined using a Zeiss Axiophot fluorescence microscope.

[^{3}H]oleic acid uptake and incorporation into cellular lipids. After serum deprivation, cells in six-well dishes were incubated for 1 h in KRBH:100 µmol/l BSA:5 mmol/l glucose with or without 174 nmol/l insulin. The assay was initiated by addition of 100 µmol/l [^{3}H]oleic acid (OA) (5 µCi per well). At various times (t), aliquots of medium were counted in duplicate, and the uptake was calculated as $(dpm_{t=0} - dpm_t)/dpm_{t=0} \times 100\%$, where dpm is the number of disintegrations per min per aliquot. After 90 min, uptake was terminated by exhaustive washing with ice-cold PBS. Cells were lysed, and an aliquot was used to determine cell-associated radioactivity by liquid scintillation counting. Total cellular lipids were extracted according to a modified Folch method (35), dried under a stream of nitrogen, dissolved in $CHCl_3$:MeOH (2:1), mixed with lipid standards for TG, diglyceride (DG), LPA, and PA, and loaded onto two thin-layer chromatography (TLC) plates. One plate was developed in $CHCl_3$:MeOH:H_2O (65:25:4), which separates polar lipids, and the other in hexane:diethyl ether:acetic acid (80:20:2), which separates neutral lipids. Individual lipid spots were visualized by exposing the dried TLC plates to iodine vapor and/or a phosphor screen (Bio-Rad, Hercules, CA), scraped from the plate, and dissolved in scintillation fluid, and radioactivity was determined by counting.

Lipid and glycogen synthesis. After serum starvation, cells in six-well dishes were incubated for 15 min in KRBH/BSA without glucose. Insulin was added for an additional 15 min. The assay was started by adding 5 mmol/l [^{14}C]glucose (1 µCi per well) to the culture medium, followed by incubation at 37°C for 1 h. Uptake was terminated by washing the cells three times with ice-cold PBS containing 10 mmol/l glucose. Cells were lysed using 1 ml RIPA (150 mmol/l NaCl:1% NP-40:0.5% deoxycholate:0.l% SDS, 50 mmol/l Tris pH 8.0) per well. Cell-associated radioactivity in 50 µl lysate was determined by liquid scintillation counting. To determine lipid-associated radioactivity, lipids were extracted from 450 µl cell lysate (35) and counted. Another aliquot of cell lysate (450 µl) was used to measure [^{14}C]glycogen formation (36).

Lipolysis assay. AGAT- or mock-transfected 3T3-L1 adipocytes grown in six-well dishes were rinsed with PBS, incubated for 3 h with 600 µmol/l OA and 300 µmol/l BSA, and washed with DMEM/300 µmol/l BSA three times. DMEM:600 µmol/l BSA:25 mmol/l HEPES (500 µl) was added to the cells, which were incubated for 30 min with or without 10 µmol/l isoproterenol. At the end of the incubation, the medium was collected, concentrated, and assayed with kits for glycerol (Sigma) and NEFA (Wako Chemicals, Richmond, VA).

AGAT activity in cell extracts. Cell extracts were prepared as previously described (37), and total protein was measured using a kit (Bio-Rad). An aliquot of cell extract (7–10 µg) was added to a reaction mixture containing 50 µmol/l LPA (oleoly-*sn*-glycero-3-phosphate) and 50 µmol/l [^{14}C]oleoyl-CoA (Amersham), followed by incubation for 3–6 min at 30°C. The reaction was terminated by spotting an aliquot onto a silica gel 60 TLC plate, which was developed in chloroform:methanol:water (65:25:4). Production of radiolabeled lipids was quantified as described above.

Statistical methods. Comparisons were performed using a two-tailed Student's t test. $P \leq 0.05$ was considered significant. Data are means ± SE.

RESULTS

Stable cell lines overexpressing human AGAT-α. Stable 3T3-L1 and C2C12 cell lines expressing His_6-tagged human AGAT-α (AGAT-) or containing vector pcDNA3.1/HisC alone (mock-) were generated. Cellular localization of the His_6-AGAT fusion protein, which has an apparent molecular mass of 34 kDa (Fig. 1), was examined in 3T3-L1 fibroblasts and adipocytes and in C2C12 myoblasts and myotubes incubated with anti-His_6 antibody. Immunofluorescence microscopy showed distinct cytoplasmic staining in all cell types (Fig. 2, left panels); staining did not occur in mock-transfected cells (Fig. 2, right panels). Overexpression of AGAT-α did not significantly alter cell morphology, cell proliferation rate, or differentiation of fibroblasts and myoblasts into adipocytes and myotubes.

Cell extracts of AGAT– and mock–3T3-L1 adipocytes or AGAT- and mock-C2C12 myotubes were assayed for the conversion of [^{14}C]oleoyl-CoA to [^{14}C]PA. The endogenous AGAT activity in 3T3-L1 adipocyte extracts was nearly an order of

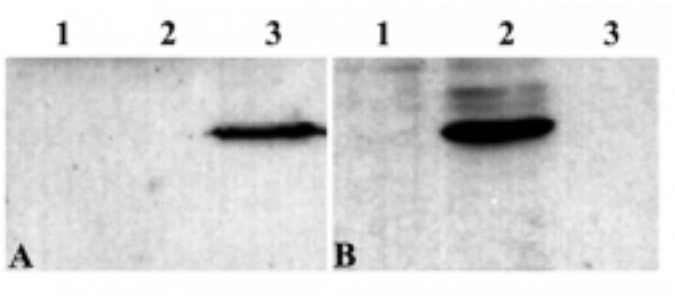

FIG. 1. Western blot analysis of stable cell lines overexpressing human AGAT-α. Cellular lysates (30–60 µg) prepared from the indicated cells were analyzed for His_6-tagged AGAT-α expression by Western blotting using a monoclonal anti-His_6 antibody as described in RESEARCH DESIGN AND METHODS. *A*: 3T3-L1 fibroblasts: *lane 1*, control (without vector); *lane 2*, mock-transfected (vector only); and *lane 3*, AGAT transfected. *B*: C2C12 myoblasts: *lane 1*, control; *lane 2*, AGAT transfected; and *lane 3*, mock transfected.

magnitude higher than that in C2C12 myotube extracts (Table 1). [^{14}C]PA formation in AGAT-C2C12 myotubes was 150% of that of the mock-transfected myotubes ($P < 0.02$). Measures of [^{14}C]PA and [^{14}C]phosphatidylethanolamine production in AGAT-overexpressing adipocyte extracts were 123% ($P < 0.04$) and 131% ($P < 0.02$) of those of mock-transfected adipocyte extracts.

Effects of AGAT-α overexpression on [^{3}H]OA and [^{14}C]glucose metabolism in 3T3-L1 adipocytes. [^{3}H]OA or [^{14}C]glucose uptake by 3T3-L1 adipocytes and C2C12 myotubes was measured as a function of insulin concentration (data not shown); the maximal [^{3}H]OA uptake (>90%) by 3T3-L1 adipocytes occurred at 10 nmol/l of insulin, and was not significantly different between 10 nmol/l and 1 µmol/l of insulin. In C2C12 myotubes, the maximal [^{14}C]glucose uptake observed was ≥174 nmol/l. When called for, insulin was used at 174 nmol/l.

[^{3}H]OA uptake in the absence and presence of insulin was measured in AGAT-L1 and mock-L1 adipocytes. At 90 min, insulin treatment enhanced [^{3}H]OA uptake in AGAT-L1 cells (65%, $P = 0.04$) and mock-L1 cells (170%, $P = 0.004$), and under both conditions, [^{3}H]OA uptake was increased by AGAT-α overexpression (by 27% with insulin treatment and by 130% without insulin treatment) (Fig. 3).

Total cellular lipids were extracted at the end of the 90-min incubation and separated by TLC (Fig. 4*A*). Radioactivity associated with LPA, PA, DG, and TG was quantified, and the incorporation of [^{3}H]OA into glycerolipids was assessed. There were no significant differences in cellular [^{3}H]LPA or [^{3}H]DG content in AGAT-L1 and mock-L1 adipocytes in the presence or absence of insulin (Fig. 4*B)*. Insulin increased [^{3}H]PA in both AGAT-L1 and mock-L1 adipocytes (40 and 107%); AGAT-α overexpression increased [^{3}H]PA under both basal and insulin-stimulated conditions (96 and 33%). Insulin increased [^{3}H]TG content in mock-L1 adipocytes (181%), but not in AGAT-L1 adipocytes; AGAT-α overexpression increased [^{3}H]TG, but only under basal conditions (196%). Under all conditions studied, most [^{3}H]OA was converted to TG.

Insulin significantly increased total glucose uptake in both AGAT-L1 and mock-L1 adipocytes (514 and 330%), and

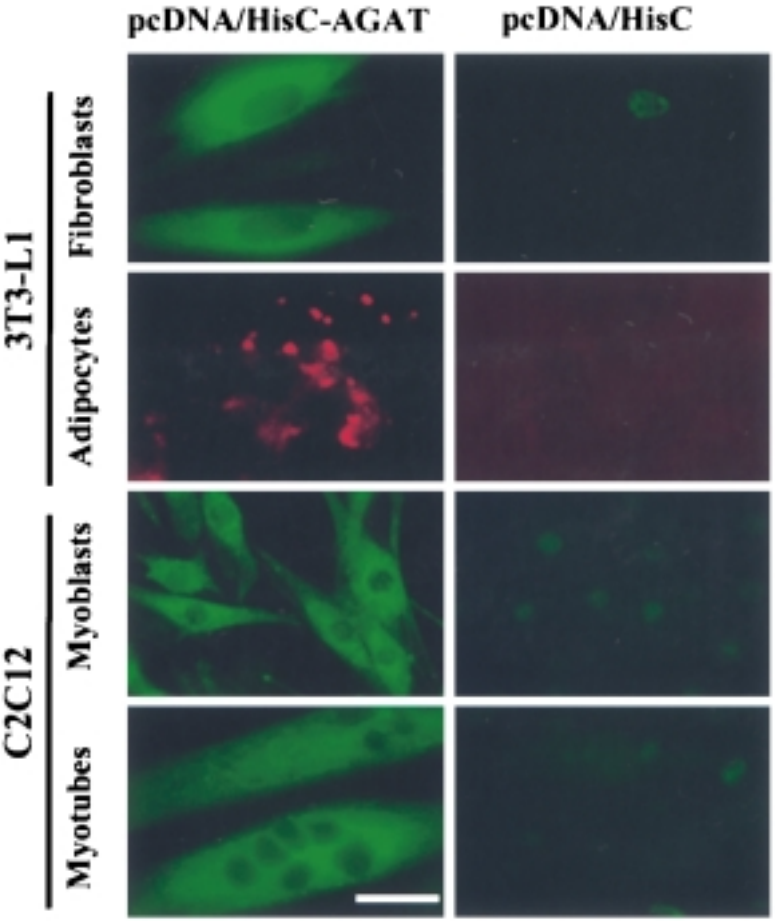

FIG. 2. Immunocytochemical staining for human AGAT-α in stable cell lines transfected with AGAT (left) or pcDNA/HisC vector (right). His_6-tagged AGAT-α was detected using an anti-His_6 primary antibody and secondary antibody conjugated by FITC, or rhodamine in the case of 3T3-L1 adipocytes. Cells were examined by Zeiss Axiophot fluorescence microscopy at 400× magnification. Scale bar, 25 µm.

TABLE 1
Glycerolipid formation in extracts of 3T3-L1 adipocytes and C2C12 myotubes

	PA (%)	PE (%)	DG + TG (%)
3T3-L1 adipocytes			
Mock	12,328 ± 664 (81 ± 4.3)	1,510 ± 83 (10.5 ± 0.5)	1,329 ± 49 (8.8 ± 0.3)
AGAT	15,187 ± 630 (100 ± 4.2)	1,978 ± 36 (13 ± 0.2)	1,321 ± 58 (8.7 ± 0.4)
P	< 0.04	< 0.02	NS
C2C12 myotubes			
Mock	1,316 ± 102 (52.2 ± 4)	541 ± 23 (21.4 ± 0.9)	666 ± 33 (26.4 ± 1.3)
AGAT	1,980 ± 12 (78.5 ± 0.5)	586 ± 22 (23.2 ± 0.9)	618 ± 12 (24.5 ± 0.5)
P	< 0.02	NS	NS

Data are means ± SE of an individual experiment performed in triplicate, and are representative of five separate experiments for C2C12 myotubes and three separate experiments for 3T3-L1 adipocytes, each experiment performed in triplicate. Cell extracts from mock– and AGAT–3T3-L1 adipocytes and C2C12 myotubes were assayed for AGAT activity. The conversion of [^{14}C]oleoyl-CoA is expressed in picomoles of [^{14}C]oleoyl-CoA incorporated per milligram of protein per minute and as a percentage of PA, PE, or DG + TG formed relative to that formed in mock-transfected cell extracts; mock (PA + PE + DG + TG) = 100%.

AGAT-α overexpression did not affect basal glucose uptake but significantly increased insulin-stimulated glucose uptake (56%) (Fig. 5*A*). These findings accorded with measurements of the conversion of glucose to cellular lipids, which significantly increased with insulin exposure in AGAT-L1 and mock-L1 cells (920 and 350%) and with AGAT-α overexpression under the condition of insulin stimulation (85%) (Fig. 5*B*).

Lipolysis and re-esterification. In the lipolysis assay, isoproterenol exposure increased glycerol release in both AGAT-L1 and mock-L1 adipocytes (37 and 40%) (Fig. 6*A*) and OA release in mock-L1 cells (120%) (Fig. 6*B*). The increase in OA release with isoproterenol in AGAT-L1 cells was substantial (105%) but not significant (Fig. 6*B*). AGAT-α overexpression affected neither basal nor isoproterenol-mediated glycerol release (Fig. 6*A*), but suppressed OA release under both conditions (–44 and –45%) (Fig. 6*B*). In the absence of NEFA re-esterification, the concentration of NEFA in the medium would be expected to be three times that of glycerol. Calculation of the percentage of NEFA relative to glycerol in the medium yielded values indicating that most of the mobilized NEFAs were re-esterified, a result enhanced by AGAT-α overexpression (Table 2).

Effect of AGAT-α overexpression on [^{14}C]glucose and [^{3}H]OA utilization in C2C12 myotubes. To identify the role of AGAT-α in the utilization of fuel molecules by skeletal muscle, the effects of AGAT-α overexpression on [^{14}C]glucose and [^{3}H]OA uptake in C2C12 myotubes were assessed in the absence and presence of insulin. Treatment of fully differentiated muscle cells with 174 nmol/l insulin did not significantly affect [^{3}H]OA uptake in either mock- or AGAT-C2C12 myotubes (Fig. 7). Similar results were observed between 1 and 500 nmol/l insulin (data not shown). AGAT overexpression increased [^{3}H]OA uptake by 34% (P = 0.027) in the presence of 174 nmol/l insulin, but not in the absence of insulin (Fig. 7).

Insulin exposure increased [^{14}C]glucose uptake in both AGAT-C2C12 and mock-C2C12 myotubes (29 and 23%), although AGAT-α overexpression did not alter either basal or insulin-stimulated glucose uptake (Fig. 8*A*). In the presence of insulin, AGAT-α overexpression altered the metabolic fate of intracellular glucose; glycogen synthesis decreased (–30%) (Fig. 8*B*), and glucose conversion to lipids increased (33%) (Fig. 8*C*).

DISCUSSION

Insulin stimulates cellular glucose uptake at multiple steps, including transport across the plasma membrane (38) and intracellular metabolism (39,40). Although overexpression of GLUT1 in skeletal muscle of transgenic mice increases cellular glucose uptake and glycogen content, intracellular glucose also accumulates (22). Thus, under conditions of increased glucose transport, cellular glucose metabolism in skeletal muscle may be rate limiting with respect to whole-body glucose disposal. Similarly, cellular metabolism of NEFA to glycerolipids, especially TG, might be the primary determinant of the rate of NEFA uptake in adipose tissue.

Although the enzymes involved in glycerolipid synthesis have been identified, the role of each enzyme in cellular TG accu-

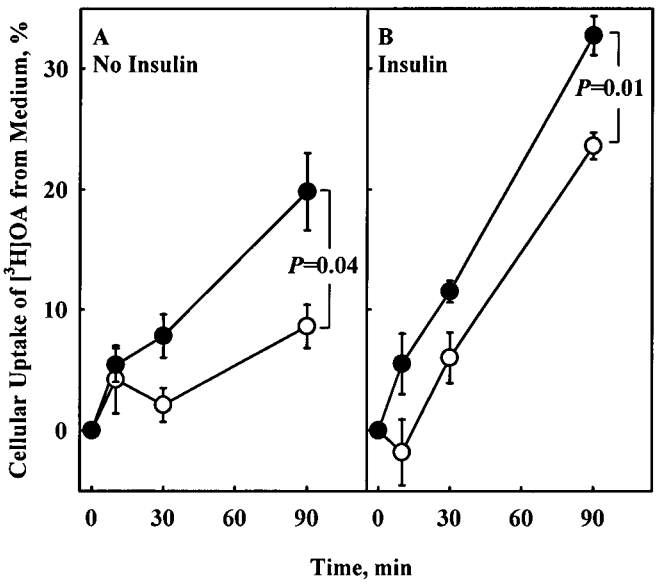

FIG. 3. [^{3}H]OA uptake in the absence (*A*) or presence (*B*) of insulin by 3T3-L1 adipocytes overexpressing human AGAT-α (●) or transfected by pcDNA/HisC vector (○). After serum starvation, adipocytes were incubated for 1 h with or without 174 nmol/l insulin, followed by incubation for 1.5 h with 1:1 [^{3}H]OA:BSA. At various times, duplicate aliquots of medium were removed, and radioactivity was determined by liquid scintillation counting. Data are means ± SE (n = 3) and are representative of two independent experiments.

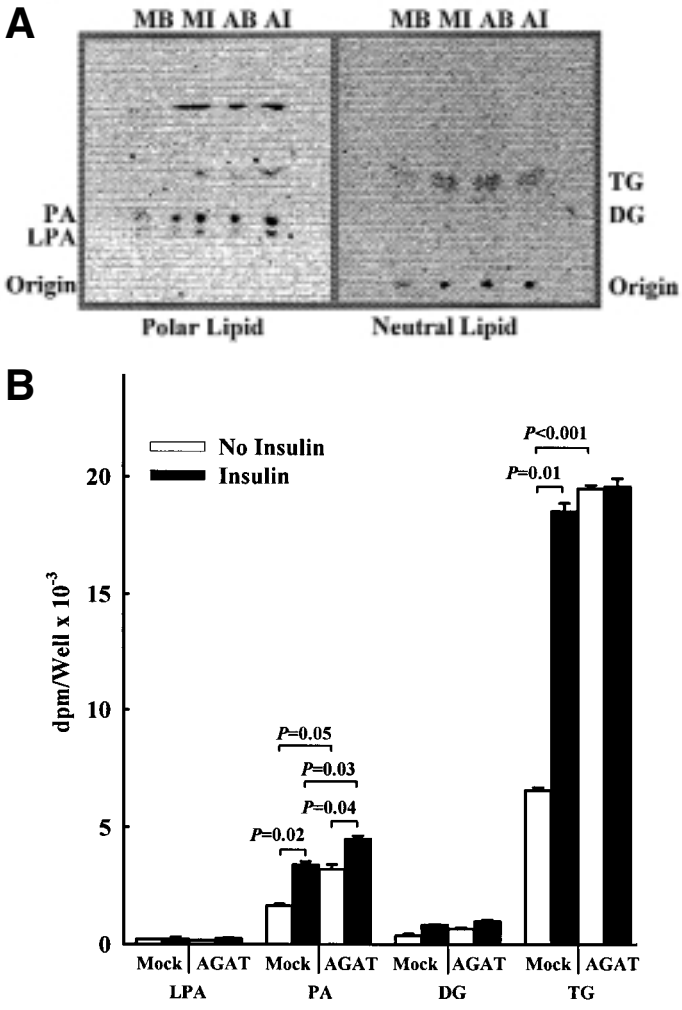

FIG. 4. Effects of AGAT overexpression and insulin treatment on the lipid profile of 3T3-L1 adipocytes. *A*: Adipocytes were treated as described in Fig. 3. Cellular lipids were extracted and analyzed by TLC as described in RESEARCH DESIGN AND METHODS. Left panel, separation of polar lipids. Right panel, separation of neutral lipids. MB, mock-transfected cells unexposed to insulin (basal); MI, mock-transfected cells incubated with insulin; AB, AGAT-transfected cells unexposed to insulin (basal); AI, AGAT-transfected cells incubated with insulin. *B*: Spots corresponding to LPA, PA, DG, and TG were transferred to vials, and the associated radioactivity was measured by liquid scintillation counting. AGAT, AGAT-transfected 3T3-L1 adipocytes; mock, mock-transfected 3T3-L1 adipocytes. Data are means ± SE of two experiments. Differences for which *P* values are not shown are not statistically significant.

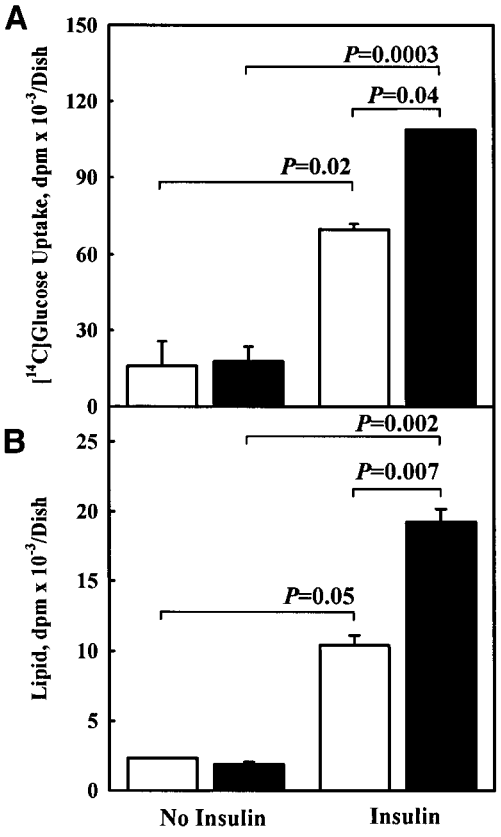

FIG. 5. [^{14}C]glucose uptake (*A*) and conversion to lipids (*B*) in AGAT-transfected (■) and mock-transfected (□) 3T3-L1 adipocytes with or without insulin incubation. For determination of glucose uptake, serum- and glucose-starved cells were incubated for 1 h with 5 mmol/l [^{14}C]glucose in KRBH:100 mmol/l BSA buffer with or without 174 nmol/l insulin and lysed. Aliquots of cellular lysate were transferred to vials and the associated radioactivity was determined by liquid scintillation counting. Cellular lipids were extracted from a second aliquot and transferred to vials for radioactivity measurement. Data are means ± SE of an individual experiment performed in triplicate and are representative of two separate experiments. Differences for which *P* values are not shown are not statistically significant.

mulation and energy uptake is unknown. We established stable 3T3-L1 and C2C12 cell lines overexpressing human AGAT-α. These cells were used to evaluate the effects of AGAT-α overexpression on cellular energy uptake and TG synthesis.

In both the presence and absence of insulin, overexpression of AGAT-α in 3T3-L1 fat cells increased OA uptake and its incorporation into TG (Figs. 3 and 4*B*). However, OA uptake was greater in the presence of insulin, suggesting that the coordinate regulation of other insulin-responsive genes can enhance the effects of AGAT-α overexpression. These genes might include those for adipocyte fatty acid binding protein (41), FACS (42), glycerol-3-phosphate acyltransferase (GPAT) (43,44), and hormone-sensitive lipase (HSL). On the other hand, in C2C12 myotubes insulin did not affect OA uptake, and AGAT-α overexpression produced only modest increases in OA uptake, which was observed only in the presence of insulin. Because AGAT activity is seven- to ninefold higher in 3T3-L1 adipocytes than in C2C12 myotubes (Table 1), it is possible that adipocytes have a higher expression of other adipogenic genes, such as FATP, FACS, GPAT, PA phosphohydrolase, and DG acyltransferase, which are required for the conversion of NEFA to TG. It is also possible that C2C12 cells lack the mechanism(s) for activating the adipogenic genes that would support increased TG synthesis and NEFA uptake.

In adipocytes, intracellular lipolysis is catalyzed by HSL, which liberates both glycerol and NEFA; this activity is stimulated by isoproterenol. The cellular release of glycerol, which cannot be directly esterified by adipocytes (45,46), provides an estimate of HSL activity. In contrast, the NEFA liberated by HSL can be either released into the medium or re-esterified, so that differences in the amount of NEFA released and the amount expected on the basis of glycerol release reflect the effects of NEFA re-esterification. Our data (Table 2 and Fig. 6) show that the amount of NEFA released

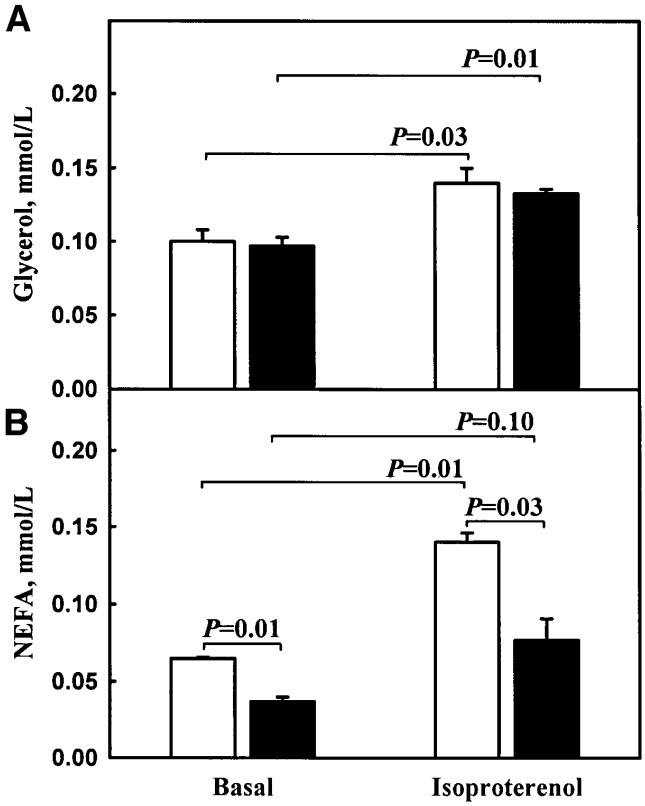

FIG. 6. Intracellular lipolysis in AGAT-transfected (■) and mock-transfected (□) 3T3-L1 adipocytes. Adipocytes were loaded with TG by incubation with OA as described in RESEARCH DESIGN AND METHODS. After the cells were washed, incubation with or without isoproterenol (10 μmol/l) was continued for 30 min. Aliquots of culture medium from each dish were collected and assayed for glycerol (*A*) and NEFA (*B*). Data are means ± SE of an individual experiment performed in triplicate and are representative of two independent experiments. Differences for which *P* values are not shown are not statistically significant.

into the medium was low relative to glycerol under all conditions studied, indicating that most NEFA liberated by HSL are re-esterified. Under both basal and isoproterenol-stimulated conditions, AGAT-α overexpression decreased NEFA release. Because AGAT overexpression increases cellular TG (Fig. 4*B*), we conclude that most of the mobilized NEFA return to the intracellular TG pool, and that AGAT-α overexpression increases esterification of NEFA derived from both intracellular lipolysis (Table 1 and Fig. 6) and the extracellular medium (Fig. 3).

TABLE 2
Percentage of NEFA released to culture medium, relative to glycerol, by 3T3-L1 adipocytes

	Transfection		
	pHis-AGAT	Mock	*P*
Basal	12	20	0.01
Isoproterenol-stimulated	20	33	0.03

Calculated as [NEFA] ÷ 3[glycerol] × 100%, where [NEFA] and [glycerol] are the molar concentrations of NEFA and glycerol in medium.

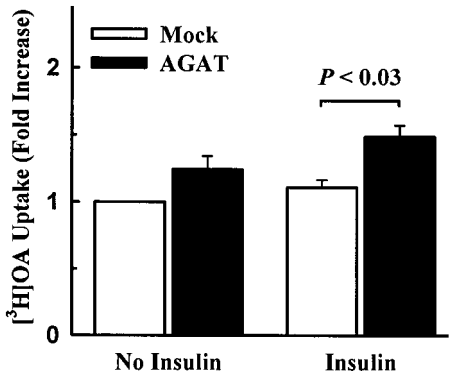

FIG. 7. [^{3}H]OA uptake by AGAT-transfected (■) or mock-transfected (□) C2C12 myotubes. [^{3}H]OA uptake assay was performed as described in RESEARCH DESIGN AND METHODS. At the end of the incubation, cells were washed extensively and lysed. Cell-associated radioactivity was determined by scintillation counting. Data are the means ± SE of three separate experiments, each performed in duplicate.

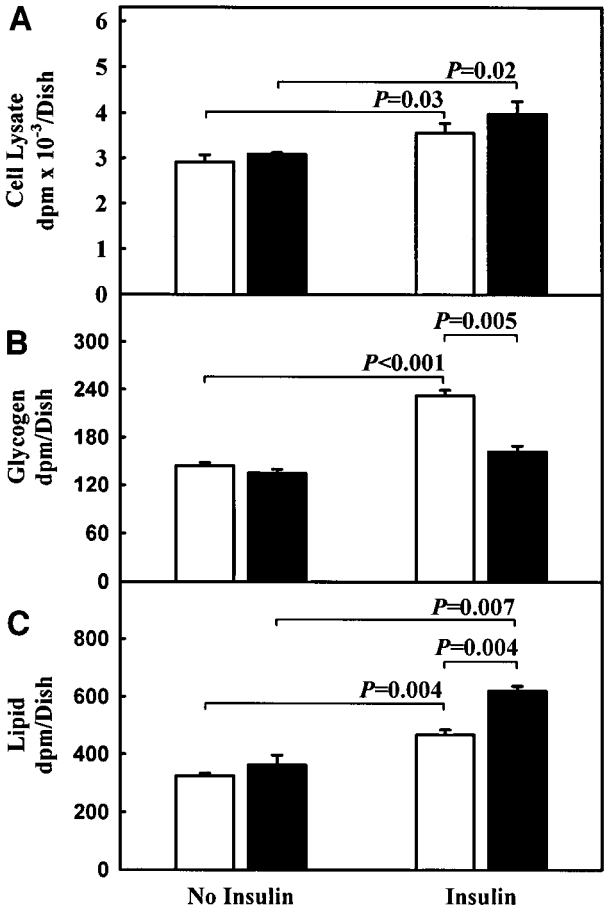

FIG. 8. [^{14}C]glucose uptake (*A*), glycogen synthesis (*B*), and lipid synthesis (*C*) in AGAT-transfected (■) and mock-transfected (□) C2C12 myotubes with or without insulin stimulation. Serum- and glucose-starved C2C12 myotubes were incubated for 1 h with 5 mmol/l [^{14}C]glucose with or without 174 nmol/l insulin. The cells were washed and lysed, and glycogen and lipids were isolated as described in RESEARCH DESIGN AND METHODS. Radioactivity was determined by liquid scintillation counting. Data are means ± SE (n = 3) and are representative of two independent experiments, each performed in triplicate. Differences for which *P* values are not shown are not statistically significant.

Cellular glucose metabolism was also altered by AGAT-α overexpression, and the alterations were different in 3T3-L1 and C2C12 cells. In 3T3-L1 fat cells, AGAT-α overexpression increased glucose uptake and its conversion to lipids, but only with insulin stimulation (Fig. 5). The absence of an effect without insulin is likely because of a strict requirement for insulin-dependent activities in the pathway that converts extracellular glucose to intracellular 1-acyl-glycerol-3-phosphate or fatty acyl CoA, the substrates for AGAT. The insulin-dependent activities may include GLUT4, hexokinase, and the enzymes involved in lipogenesis, such as acetyl-CoA carboxylase, pyruvate dehydrogenase, and fatty acid synthase (47). Similarly, in C2C12 cells, AGAT-α overexpression had no effect on basal glucose uptake. In the presence of insulin, however, AGAT-α overexpression diverted glucose from glycogen synthesis to lipid synthesis (Fig. 8*B* and *C*), presumably because of increased entry of glucose-6-phosphate into the glycolysis pathway generating acetyl-CoA and glycerol-3-phosphate.

Because AGAT catalyzes the conversion of LPA to PA (31), AGAT overexpression in 3T3-L1 adipocytes would be expected to increase cellular PA content. However, in our experiments, that difference was small; the greatest difference was in cellular TG content. In contrast to the intact cells, most of the product formed in cell extracts was PA (Table 1), and AGAT overexpression only modestly increased PA and did not increase TG formation. This finding is consistent with a model in which AGAT is proximal to the other enzymes of glycerolipid synthesis. Disruption of cells could separate these enzymes and uncouple their activities. Consequently, PA accumulates in the extracts, but not in intact AGAT-L1 adipocytes.

In 3T3-L1 adipocytes, AGAT-α overexpression increases NEFA uptake and decreases NEFA efflux. Increased entry of NEFA into the glycerolipid synthesis pathway would lower the cytoplasmic NEFA concentration and in turn create a NEFA concentration gradient across the plasma membrane. This gradient could drive NEFA influx, which may be diffusive (48,49) or involve NEFA transport proteins (30). In a physiological context, increased AGAT activity in adipose tissue might decrease plasma NEFA concentrations. Future studies of this pathway should include tests of AGAT overexpression in vivo to determine whether it is an attractive target for pharmacological management of plasma NEFA and lipoprotein concentrations.

ACKNOWLEDGMENTS

This work was supported by grants from the National Institutes of Health (HL-30914 and HL-56865) and the Ethel L. Walker Memorial Research and Education Fund for Arteriosclerosis. H.R. was a student in The Michael E. DeBakey Graduate Program in Cardiovascular Sciences.

REFERENCES

1. Randle P, Garland P, Hales C, Newsholme E: The glucose fatty-acid cycle: its role in insulin sensitivity and the metabolic disturbances of diabetes mellitus. *Lancet* 1:785–789, 1963
2. McGarry JD: What if Minkowski had been ageusic?: An alternative angle on diabetes. *Science* 258:766–770, 1992
3. Roden M, Price TB, Perseghin G, Petersen KF, Rothman DL, Cline GW, Shulman GI: Mechanism of free fatty acid-induced insulin resistance in humans. *J Clin Invest* 97:2859–2865, 1996
4. Boden G, Chen X, Ruiz J, White JV, Rossetti L: Mechanisms of fatty acid-induced inhibition of glucose uptake. *J Clin Invest* 93:2438–2446, 1994
5. Ferrannini E, Barrett EJ, Bevilacqua S, DeFronzo RA: Effect of fatty acids on glucose production and utilization in man. *J Clin Invest* 72:1737–1747, 1983
6. Ruderman NB, Toews CJ, Shafrir E: Role of free fatty acids in glucose homeostasis. *Arch Intern Med* 123:299–313, 1969
7. Byrne CD, Brindle NP, Wang TW, Hales CN: Interaction of non-esterified fatty acid and insulin in control of triacylglycerol secretion by Hep G2 cells. *Biochem J* 280:99–104, 1991
8. Laws A: Free fatty acids, insulin resistance and lipoprotein metabolism. *Curr Opin Lipidol* 7:172–177, 1996
9. Reaven GM, Chang H, Ho H, Jeng CY, Hoffman BB: Lowering of plasma glucose in diabetic rats by antilipolytic agents. *Am J Physiol* 254:E23–E30, 1988
10. Reaven GM, Chang H, Hoffman BB: Additive hypoglycemic effects of drugs that modify free-fatty acid metabolism by different mechanisms in rats with streptozocin-induced diabetes. *Diabetes* 37:28–32, 1988
11. Balasse EO, Neef MA: Influence of nicotinic acid on the rates of turnover and oxidation of plasma glucose in man. *Metabolism* 22:1193–1204, 1973
12. Saloranta C, Franssila-Kallunki A, Ekstrand A, Taskinen MR, Groop L: Modulation of hepatic glucose production by non-esterified fatty acids in type 2 (non-insulin-dependent) diabetes mellitus. *Diabetologia* 34:409–415, 1991
13. Boden G, Chen X, Iqbal N: Acute lowering of plasma fatty acids lowers basal insulin secretion in diabetic and nondiabetic subjects. *Diabetes* 47:1609–1612, 1998
14. Shulman GI, Rothman T, Jue P, Stein RA, DeFronzo RA, Shulman RG: Quantitation of muscle glycogen synthesis in normal subjects and subjects with non-insulin-dependent diabetes by ^{13}C nuclear magnetic resonance spectroscopy. *N Engl J Med* 322:223–228, 1990
15. Oscai LB, Essig DA, Palmer WK: Lipase regulation of muscle triglyceride hydrolysis. *J Appl Physiol* 69:1571–1577, 1990
16. Falholt K, Jensen I, Lindkaer Jensen S, Mortensen H, Volund A, Heding LG, Petersen PN, Falholt W: Carbohydrate and lipid metabolism of skeletal muscle in type 2 diabetic patients. *Diabet Med* 5:27–31, 1988
17. Man ZW, Hirashima T, Mori S, Kawano K: Decrease in triglyceride accumulation in tissues by restricted diet and improvement of diabetes in Otsuka Long-Evans Tokushima fatty rats, a non-insulin-dependent diabetes model. *Metabolism* 49:108–114, 2000
18. Storlien LH, Jenkins AB, Chisholm DJ, Pascoe WS, Khouri S, Kraegen EW: Influence of dietary fat composition on development of insulin resistance in rats: relationship to muscle triglyceride and omega-3 fatty acids in muscle phospholipid. *Diabetes* 40:280–289, 1991
19. Pan DA, Lillioja S, Kriketos AD, Milner MR, Baur LA, Bogardus C, Jenkins AB, Storlien LH: Skeletal muscle triglyceride levels are inversely related to insulin action. *Diabetes* 46:983–988, 1997
20. Lawrence JC Jr, Piper RC, Robinson LJ, James DE: GLUT4 facilitates insulin stimulation and cAMP-mediated inhibition of glucose transport. *Proc Natl Acad Sci U S A* 89:3493–3497, 1992
21. Ren JM, Marshall BA, Mueckler MM, McCaleb M, Amatruda JM, Shulman GI: Overexpression of Glut4 protein in muscle increases basal and insulin-stimulated whole body glucose disposal in conscious mice. *J Clin Invest* 95:429–432, 1995
22. Ren JM, Marshall BA, Gulve EA, Gao J, Johnson DW, Holloszy JO, Mueckler M: Evidence from transgenic mice that glucose transport is rate-limiting for glycogen deposition and glycolysis in skeletal muscle. *J Biol Chem* 268: 16113–16115, 1993
23. Chang PY, Jensen J, Printz RL, Granner DK, Ivy JL, Moller DE: Overexpression of hexokinase II in transgenic mice: evidence that increased phosphorylation augments muscle glucose uptake. *J Biol Chem* 271:14834–14839, 1996
24. Manchester J, Skurat AV, Roach P, Hauschka SD, Lawrence JC Jr: Increased glycogen accumulation in transgenic mice overexpressing glycogen synthase in skeletal muscle. *Proc Natl Acad Sci U S A* 93:10707–10711, 1996
25. Cheung JY, Conover C, Regen DM, Whitfield CF, Morgan HE: Effect of insulin on kinetics of sugar transport in heart muscle. *Am J Physiol* 234:E70–E78, 1978
26. Manchester J, Kong X, Nerbonne J, Lowry OH, Lawrence JC Jr: Glucose transport and phosphorylation in single cardiac myocytes: rate-limiting steps in glucose metabolism. *Am J Physiol* 266:E326–E333, 1994
27. Kubo K, Foley JE: Rate-limiting steps for insulin-mediated glucose uptake into perfused rat hindlimb. *Am J Physiol* 250:E100–E102, 1986
28. Yki-Jarvinen H, Young AA, Lamkin C, Foley JE: Kinetics of glucose disposal in whole body and across the forearm in man. *J Clin Invest* 79:1713–1719, 1987
29. Katz A, Sahlin K, Broberg S: Regulation of glucose utilization in human skeletal muscle during moderate dynamic exercise. *Am J Physiol* 260:E411–E415, 1991
30. Schaffer JE, Lodish HF: Expression cloning and characterization of a novel adipocyte long chain fatty acid transport protein. *Cell* 79:427–436, 1994
31. Brindley DN: Metabolism of triacylglycerols. In *Biochemistry of Lipids, Lipoproteins, and Membranes: New Comprehensive Biochemistry*. Vol. 20. Vance DE, Vance JE, Eds. Amsterdam, Elsevier Science, 1991, p. 171–203

32. West J, Tompkins CK, Balantac N, Nudelman ED, Meengs B, White T, Bursten S, Coleman J, Kumar A, Singer JW, Leung DW: Cloning and expression of two human lysophosphatidic acid acyltransferase cDNAs that enhance cytokine-induced signaling responses in cells. *DNA Cell Biol* 16:691–701, 1997
33. Student AK, Hsu RY, Lane MD: Induction of fatty acid synthetase synthesis in differentiating 3T3-L1 preadipocytes. *J Biol Chem* 255:4745–4750, 1980
34. Coleman J: Characterization of *Escherichia coli* cells deficient in 1-acyl-*sn*-glycerol-3- phosphate acyltransferase activity. *J Biol Chem* 265:17215–17221, 1990
35. Hamilton S, Hamilton RJ, Sewell PA: Extraction of lipids and derivative formation. In *Lipid Analysis: A Practical Approach*. Hamilton RJ, Hamilton S, Eds. Oxford, NY, IRL Press at Oxford University Press, 1992, p. 13–64
36. Hess SL, Suchin CR, Saltiel AR: The specific protein phosphatase inhibitor okadaic acid differentially modulates insulin action. *J Cell Biochem* 45:374–380, 1991
37. Harlow E, Lane D: *Antibodies: A Laboratory Manual*. Cold Spring Harbor, NY, Cold Spring Harbor Laboratory, 1988, p. 451
38. Kahn BB: Lilly Lecture 1995: Glucose transport: pivotal step in insulin action. *Diabetes* 45:1644–1654, 1996
39. Pendergrass M, Koval J, Vogt C, Yki-Jarvinen H, Iozzo P, Pipek R, Ardehali H, Printz R, Granner D, DeFronzo RA, Mandarino LJ: Insulin-induced hexokinase II expression is reduced in obesity and NIDDM. *Diabetes* 47:387–394, 1998
40. Lawrence JC Jr, Skurat AV, Roach PJ, Azpiazu I, Manchester J: Glycogen synthase: activation by insulin and effect of transgenic overexpression in skeletal muscle. *Biochem Soc Trans* 25:14–19, 1997
41. Melki SA, Abumrad NA: Expression of the adipocyte fatty acid-binding protein in streptozotocin-diabetes: effects of insulin deficiency and supplementation. *J Lipid Res* 34:1527–1534, 1993
42. Weiner FR, Smith PJ, Wertheimer S, Rubin CS: Regulation of gene expression by insulin and tumor necrosis factor alpha in 3T3-L1 cells: modulation of the transcription of genes encoding acyl-CoA synthetase and stearoyl-CoA desaturase-1. *J Biol Chem* 266:23525–23528, 1991
43. Shin DH, Paulauskis JD, Moustaid N, Sul HS: Transcriptional regulation of p90 with sequence homology to *Escherichia coli* glycerol-3-phosphate acyltransferase. *J Biol Chem* 266:23834–23839, 1991
44. Jerkins AA, Liu WR, Lee S, Sul HS: Characterization of the murine mitochondrial glycerol-3-phosphate acyltransferase promoter. *J Biol Chem* 270: 1416–1421, 1995
45. Shapiro B, Chowers I, Rose G: Fatty acid uptake and esterification in adipose tissue. *Biochim Biophys Acta* 23:115–120, 1957
46. Cahill GFJ, Leboeuf B, Renold AE: Factors concerned with the regulation of fatty acid metabolism by adipose tissue. *Am J Clin Nutr* 8:733–739, 1960
47. Kruszynska YT: Normal metabolism: the physiology of fuel homoeostasis. In *Textbook of Diabetes*. Vol. 1, 2nd ed. Pickup JC, Williams G, Eds. Oxford, Blackwell Science, 1997, 11.1–11.37
48. Hamilton JA: Fatty acid transport: difficult or easy? *J Lipid Res* 39:467–481, 1998
49. Civelek VN, Hamilton JA, Tornheim K, Kelly KL, Corkey BE: Intracellular pH in adipocytes: effects of free fatty acid diffusion across the plasma membrane, lipolytic agonists, and insulin. *Proc Natl Acad Sci U S A* 93:10139–10144, 1996